Magnetic field imaging with atomic Rb vapor

Eugeniy E. Mikhailov,[1] I. Novikova,[1,*] M. D. Havey,[2] and F. A. Narducci[3]

[1]*Department of Physics, The College of William & Mary, Williamsburg, Virginia 23187, USA*
[2]*Department of Physics, Old Dominion University, Norfolk, Virginia 23529, USA*
[3]*EO Sensors Division, Naval Air Systems Command, Patuxent River, Maryland 20670, USA*
**Corresponding author: inovikova@physics.wm.edu*

Received September 4, 2009; revised September 30, 2009; accepted October 6, 2009;
posted October 16, 2009 (Doc. ID 116764); published November 11, 2009

We demonstrate the possibility of dynamic imaging of magnetic fields using electromagnetically induced transparency in an atomic gas. As an experimental demonstration we employ an atomic Rb gas confined in a glass cell to image the transverse magnetic field created by a long straight wire. In this arrangement, which clearly reveals the essential effect, the field of view is about 2×2 mm^2 and the field detection uncertainty is 0.14 mG per 10 μm$\times$10 μm image pixel. © 2009 Optical Society of America

OCIS codes: 270.1670, 020.1670, 020.3690, 020.7490.

Efforts to develop measurement techniques for precision magnetometry have a long and successful history in atomic physics [1–5], including successful realizations of large-scale magnetic field imagers for clinical applications [6,7]. Here, we propose the idea of a compact high-resolution magnetometer for dynamic imaging of magnetic field gradients that takes advantage of the unique properties of the electromagnetically induced transparency (EIT) effect and the existence of coherently produced optical dark states, which can be extremely sensitive to external fields [8]. We experimentally demonstrate the essential idea with a one-axis (two-dimensional) prototype. A fully implemented three-dimensional magnetic gradiometer promises both high precision and useful visualization tools for both static and dynamic magnetically complex environments. Also, the proposed method is simple enough (only one laser field with no additional rf fields) to be implemented for remote sensing with optical fiber connections. The potential applications of this technique range from essentially fundamental (e.g., precision searches for magnetic monopoles [9]) to quite applied, for example, high-resolution real-time monitoring of the local magnetic environment in medical applications or quantum information experiments.

The proposed approach relies on the spectrally ultranarrow transmission resonances observed under EIT conditions in an atomic gas. These resonances are associated with the coherent noninteracting (dark) states in a three-level Λ system formed under the combined action of two electromagnetic fields in two-photon Raman resonance with two long-lived metastable states of an atom. The width of the EIT resonances is determined by the intensities of the laser field and the lifetime of the ground-state coherence, and can be as small as a few hertz [10,11]. Such spectral sensitivity makes this effect very promising for precision metrology. The spectral location of the transparency resonance depends on the external magnetic field when the Λ system is based on the magnetic-field-sensitive Zeeman sublevels. If the magnetic field is spatially varying transversely in a plane orthogonal to the probe beam's $\mathbf{k}$ vector, the resonances will occur at different spatial locations for different two-photon resonance detunings. Thus, the spatial distribution of transmitted intensity will display a transverse image of the spatial regions where the two-photon resonance condition is satisfied. Recording a series of such images for various two-photon frequencies can create a spatial map of the transverse magnetic field.

To reconstruct magnetic field gradients in three dimensions, one has to combine independent transmission measurements made in three orthogonal directions. That will allow six elements of the $\nabla\mathbf{B}$ tensor to be found using a known shape of EIT resonance. According to the source free Maxwell's equations, there are four constraints on the nine components of $\nabla\mathbf{B}$, implying a desirable unit redundancy in each set of measurements. Simultaneous recording of transmission and spontaneous emission along the cell [12] may provide additional information about transverse and longitudinal field gradients.

In this Letter, we illustrate the concept by imaging the magnetic field produced by a long straight wire carrying a steady current I running along the length of a Rb vapor cell. Since in our experiment we are able to detect the light transmission through the cell only in one direction, we took extreme care to make the wire as coaxial as possible with the laser beam to remove any variation in the magnetic field along the optical axis. The aim is then to measure the resulting transverse variation in the magnetic field across the laser beam by imaging the transverse variations in the transmitted light intensity as a function of the two-photon detuning.

A schematic of the experimental setup is shown in Fig. 1(a). We use a vertical-cavity surface-emitting laser (VCSEL) directly phase modulated at 6.834 GHz (the ^{87}Rb hyperfine frequency), and use the fundamental (carrier) laser frequency and one of the sidebands to produce the two optical fields required for EIT observation. The laser beam with total power 200 μW and a slightly elliptical Gaussian profile (1.8 mm and 1.4 mm FWHM), was directed into the cylindrical Pyrex cell (length 75 mm and diameter 22 mm) containing isotopically enriched ^{87}Rb vapor and 15

 © 2009 Optical Society of America

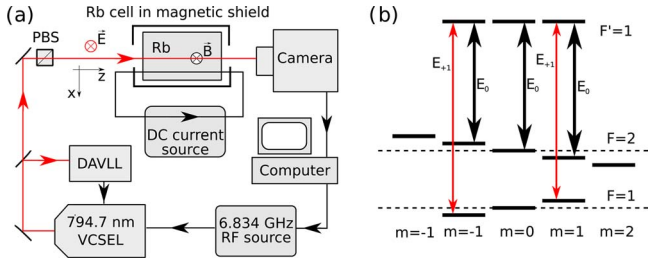

Fig. 1. (Color online) (a) A schematic diagram of the experiment. (b) Energy level diagram showing two EIT Λ schemes formed by the carrier E_0 and the first modulation sideband E_{+1}.

Torr of Ne buffer gas. The cell was mounted inside a three-layer magnetic shielding and actively maintained at 322 K.

The magnetic field-producing wire was mounted parallel to the laser beam at a distance $\rho_0 = 20.1 \pm 0.2$ mm, and connected to a low-noise current supply operating at $I = 438 \pm 1$ mA. If we let the laser beam's wave vector and the direction of current flow define the z direction, the curves of constant magnetic field B are then circles in the x–y plane and centered on the wire. For a given two-photon detuning the EIT resonance conditions are obeyed only for a given value of the magnetic field, and thus for a large laser beam we in general expect to observe a corresponding "bright" circular arc in the transmission spatial profile, with the radius of the arc depending on the set two-photon detuning. In our experimental arrangements, however, the laser beam diameter is small compare with the distance to the wire ρ_0, so the magnetic field across the laser beam is mainly along the y axis and changes linearly with small displacement δx,

$$B(\rho) = \frac{\mu_o I}{2\pi(\rho + \delta x)} \simeq \frac{\mu_o I}{2\pi\rho_0}\left(1 - \frac{\delta x}{\rho_0}\right), \qquad (1)$$

where μ_0 is permeability of free space, and we neglect the effects of the surrounding magnetic shielding. For the measurements, the laser frequency was tuned such that the stronger optical field (unmodulated carrier) was resonant with the $5S_{1/2}F=2 \rightarrow 5P_{1/2}F'=1$ transition of ^{87}Rb, while the frequency of the +1 modulation sideband matched the $5S_{1/2}$ $F=1 \rightarrow 5P_{1/2}F'=1$ transition. The laser output was linearly polarized. In this configuration there are two possible Λ systems for $F=1,2$; $m_F=\pm 1 \rightarrow F'=1$; $m_{F'}=\pm 1$ that produce EIT resonances at two-photon detunings $\Delta\nu = \Delta_{HFS} \pm 2g_m B$ [Fig. 1(b)], where $g_m = 0.7$ MHz/G is the gyromagnetic ratio for ^{87}Rb [13]. We also adjusted the power of the VCSEL modulation signal to cancel the light shift of the EIT resonances and to avoid the effects of nonuniform spatial intensity distribution of the laser beam [14]. For our experiment the cancellation occurred for a sideband/carrier intensity ratio of 0.75.

To map spatial variations in the magnetic field, we stepped the VCSEL modulation frequency in a 20 kHz range around one of the EIT resonances in 200 Hz increments, taking images of the transmitted laser beam profile using a digital camera. The dominant source of noise in our experiment was due to the phase-to-amplitude noise conversion of the VCSEL large phase noise (the linewidth of the laser was ≈100 MHz) by absorption in the cell. To reduce the detection noise of the image, we recorded and averaged 200 sequential images grabbed at a 30 frame per second rate for any particular two photon detuning. Even then the detection noise is larger than the digital resolution of the 12 bit analog-to-digital converter of the camera. For each pixel we plotted the intensity as a function of two-photon detuning [Fig. 2(a)], and located the position of the EIT maximum. After analyzing the transmission at each pixel we obtained a spatial map of magnetic field, shown in Fig. 2(b). The average variance between two sequential runs allowed us to put an upper limit on the uncertainty of the magnetic field measurements $\Delta B = 0.14$ mG for every 10 μm pixel.

We compared the measured magnetic field with numerical calculation of the magnetic field generated by a long straight wire inside a cylindrical magnetic shield. Since the inner shield modifies the magnetic field from the simple Biot–Savart law, we used a finite element (FEM) analysis program to calculate the expected magnetic field distribution inside the laser beam [15], as shown in Fig. 2(c). The rather large uncertainty of our FEM model is governed by possible variations in each shield's diameter, thickness, and

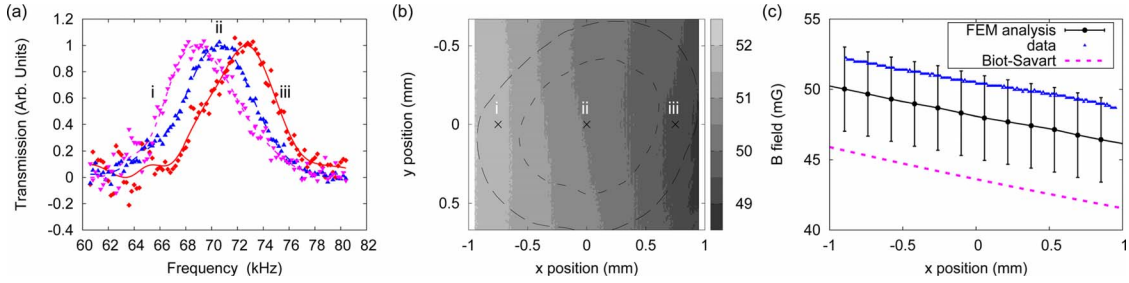

Fig. 2. (Color online) (a) Transmission through the cell detected at three different camera pixels [marked in (b)] as functions of the two-photon detuning. Solid lines show low-pass filtered data used to determine the maximum transmission frequency. (b) Map of the magnetic field strength. Dashed lines mark the 75% and 50% levels of the maximum laser beam intensity. (c) Experimentally measured magnetic field slice of the map (b) along $y=0$ as a function of x position, and the theoretically calculated magnetic fields using the Biot–Savart law and a finite element analysis. The error bars in the FEM curve represent the variation in the calculated magnetic field due to ±1 mm uncertainty in the magnetic shielding position with respect to the wire and the laser beam.

imperfect cylindrical shapes as well as the uncertainty in the location of the wire inside the shielding. For instance, Fig. 2(c) illustrates that displacement of the shielding position as small as 1 mm is sufficient to match the FEM simulations with the measurements.

The demonstrated sensitivity of our apparatus ($\approx 14\ \mu G/\mu m$) is limited by the transmitted intensity fluctuations of the broadband VCSEL output. We expect much better sensitivity for narrow-band electromagnetic fields, which should dramatically reduce the amount of amplitude noise in the output, such as a narrowband external-cavity diode laser followed by an external phase modulator. The spatial resolution is also limited by random thermal motion of atoms. For 15 Torr of Ne buffer gas, the transport mean-free path of Rb atoms is $\lambda = 3D/v_T \simeq 11\ \mu m$ [16], where D is the diffusion constant, inversely proportional to the buffer gas pressure, and v_T is average speed of Rb atoms. This diffusion length may be decreased by 1 order of magnitude in a cell with higher buffer gas pressure without significant degradation of EIT resonance characteristics [11,17].

We can estimate the precision of the magnetic field measurements ΔB owing to the uncertainty in the two-photon detuning frequency corresponding to maximum transmission for a given signal-to-noise ratio S/N [18],

$$\Delta B \simeq \frac{1}{2g_m}\frac{\gamma}{S/N\sqrt{n}}. \quad (2)$$

In this expression we assume that the EIT resonance has Lorentzian shape with a known FWHM γ, and n is the number of sampling points per resonance width. The optimal frequency span in this case should be more or equal to the value γ, with $n > 5-10$ for each recorded trace to avoid numerical errors in fitting related to discretization artifacts. If limited by camera signal-to-noise ratio (1:4096 for our 12-bit camera), the best expected sensitivity is $\Delta B \lesssim 1\ \mu G$. Improvement of 1 order of magnitude can be achieved by using 16-bit resolution cameras.

We note that the ultimate relative sensitivity of our method should be similar to that of atomic clocks, based on the same operational principle [19]. Miniature atomic clocks demonstrate a fractional stability of the order of $10^{-11}-10^{-12}/\sqrt{\text{Hz}}$. In practice the performance of the magnetic field imager may be limited by other factors, such as digital noise or the limited optical sensitivity per pixel of a charge-coupled camera. These and other factors, including the essential role of longitudinally varying magnetic fields, are currently under investigation.

In conclusion, we propose what we believe to be a new method of dynamic imaging of a magnetic field by detecting spatial and temporal variations in transmission of light through an atomic sample under conditions of electromagnetically induced transparency. This method can potentially produce three-dimensional magnetic field maps. To demonstrate the basic operational principle, we reconstructed the spatial distribution of the transverse magnetic field created by a current-carrying long straight wire, running along an atomic Rb vapor cell, with the precision of $14\ \mu G/\mu m$ inside the $1.8 \times 1.4\ mm^2$ laser beam cross-section. Our prototype apparatus can be readily scaled up for either a larger or smaller detection area by adding a zooming telescope in front of the camera. We also expect that this method can be used with recently developed chip-scale atomic clocks and magnetometers [20].

The authors thank D. Malyarenko, S. Aubin, and J. P. Davis for valuable contributions. This research was supported by NSF grants PHY-0758010 and PHY-0654226, Jeffress Research grant J-847, ONR grants N0001409WX20679 and an In-House Laboratory Innovative Research (ILIR).

References and Notes

1. D. Budker and M. V. Romalis, Nat. Phys. **3**, 227 (2007).
2. C. Affolderbach, M. Stähler, S. Knappe, and R. Wynands, Appl. Phys. B **75**, 605 (2002).
3. I. K. Kominis, T. W. Kornack, J. C. Allred, and M. V. Romalis, Nature **422**, 596 (2003).
4. S. Xu, S. M. Rochester, V. V. Yashchuk, M. H. Donaldson, and D. Budker, Rev. Sci. Instrum. **77**, 083106 (2006).
5. M. Vengalattore, J. M. Higbie, S. R. Leslie, J. Guzman, L. E. Sadler, and D. M. Stamper-Kern, Phys. Rev. Lett. **98**, 200801 (2007).
6. H. Xia, A. Ben-Amar Baranga, D. Hoffman, and M. V. Romalis, Appl. Phys. Lett. **89**, 211104 (2006).
7. G. Bison, N. Castagna, A. Hofer, P. Knowles, J.-L. Schenker, and A. Weis, arXiv:0906.4869.
8. M. Fleischhauer, A. Imamoglu, and J. P. Marangos, Rev. Mod. Phys. **77**, 633 (2005).
9. P. A. M. Dirac, Proc. R. Soc. London, Ser. A **133**, 60 (1931).
10. D. Budker, V. Yashchuk, and M. Zolotorev, Phys. Rev. Lett. **81**, 5788 (1998).
11. M. Erhard and H. Helm, Phys. Rev. A **63**, 043813 (2001).
12. H. Asahi, K. Motomura, K. Harada, and M. Mitsunaga, Opt. Lett. **28**, 1153 (2003).
13. For arbitrary orientation of the laser polarization with respect of the magnetic field vector the analysis of relative amplitudes of EIT resonances at $0, \pm g_m B$ and $\pm 2g_m B$ two-photon detunings may allow measurements of both magnitude and direction of a magnetic field.
14. S. A. Zibrov, I. Novikova, D. F. Phillips, R. L. Walsworth, A. S. Zibrov, V. L. Velichansky, A. V. Taichenachev, and V. I. Yudin, arXiv:0910.4703 (2009).
15. http://femm.foster-miller.net/wiki/HomePage.
16. W. Happer, Rev. Mod. Phys. **44**, 169 (1972).
17. S. Knappe, L. Hollberg, and J. Kitching, Opt. Lett. **29**, 388 (2004).
18. A. G. Marshall and F. R. Verdun, *Fourier Transforms in NMR, Optical, and Mass Spectrometry* (Elsevier, 1990).
19. J. Vanier, Appl. Phys. B **81**, 421 (2005).
20. V. Shah, S. Knappe, P. D. D. Schwindt, and J. Kitching, Nat. Photonics **1**, 649 (2007).